Title: JAK2 regulates mismatch repair protein-mediated epigenetic alterations in response to oxidative damage

Running title: JAK2 regulates epigenetic responses

Ning Ding[1], Sam A. Miller[1, 2], Sudha S. Savant[1], Heather M. O'Hagan[1, 3]*

[1]Medical Sciences, Indiana University School of Medicine, Bloomington, Indiana, United States of America. 47405

[2]Genome, Cell, and Developmental Biology, Department of Biology, Indiana University Bloomington, Indiana, United States of America. 47405

[3]Indiana University Melvin and Bren Simon Cancer Center, Indianapolis, Indiana, United States of America. 46202

*Corresponding author:

1001 East 3rd Street

Jordan Hall Room 108

Bloomington, IN 47405, USA

Tel: +1-812-855-3035. Fax: +1-812-855-4436

E-mail: hmohagan@indiana.edu.

Keywords: JAK2, oxidative damage, MSH2, MSH6, DNMT1, EZH2

This is the author's manuscript of the article published in final edited form as:

Ding, N., Miller, S. A., Savant, S. S., & O'Hagan, H. M. (2019). JAK2 regulates mismatch repair protein-mediated epigenetic alterations in response to oxidative damage. Environmental and Molecular Mutagenesis, 0(ja). https://doi.org/10.1002/em.22269

Abstract

At sites of chronic inflammation epithelial cells undergo aberrant DNA methylation that contributes to tumorigenesis. Inflammation is associated with an increase in reactive oxygen species (ROS) that cause oxidative DNA damage, which has also been linked to epigenetic alterations. We previously demonstrated that in response to ROS, mismatch repair (MMR) proteins MSH2 and MSH6 recruit epigenetic silencing proteins DNA methyltransferase 1 (DNMT1) and Polycomb repressive complex 2 (PRC2) members to sites of DNA damage, resulting in transcriptional repression of tumor suppressor genes (TSGs). However, it was unclear what signal is unique to ROS that results in the chromatin binding of MSH2 and MSH6. Herein, we demonstrate that in response to hydrogen peroxide (H_2O_2), JAK2 localizes to the nucleus and interacts with MSH2 and MSH6. Inhibition or knockdown of JAK2 reduces the H_2O_2-induced chromatin interaction of MSH2, MSH6, DNMT1 and PRC2 members, reduces H_2O_2-induced global increase in trimethylation of lysine 27 of histone H3 (H3K27me3), and abrogates oxidative damage-induced transcriptional repression of candidate TSGs. Moreover, JAK2 mRNA expression is associated with CpG island methylator phenotype (CIMP) status in human colorectal cancer. Our findings provide novel insight into the connection between kinase activation and epigenetic alterations during oxidative damage and inflammation.

Introduction

Chronic inflammation and the associated reactive oxygen species (ROS) play an important role in the initiation and progression of many human epithelial cancers (Ding et al. 2017). Aberrant silencing of key genes by promoter CpG island DNA hypermethylation and repressive histone modifications occurs in many cancers that form at sites of chronic inflammation (Takeshima et al. 2015) (Kondo 2009). Yet, the role inflammation plays in initiating these aberrant epigenetic alterations is not completely understood.

Epigenetic alterations cause mitotically heritable changes in gene expression without altering the DNA sequence. Aberrant epigenetic alterations promote the progression of cancer by altering the expression pattern of key tumor-related genes (Sharma et al. 2010). DNA hypermethylation of promoter CpG islands impairs transcription factor binding and thereby decreases gene expression. Post-translational modification of histone tails alters gene expression by regulating chromatin structure or recruitment of additional histone modifiers and/or readers. During chromatin-based processes such as transcription, DNA replication, and DNA repair, chromatin is modified by histone modifying enzymes, chromatin remodelers and DNA methyltransferases (Bannister and Kouzarides 2011). For instance, Polycomb repressive complex 2 (PRC), which includes Enhancer of zeste homolog 2 (EZH2), Suppressor of zeste 12 protein homolog (SUZ12), and Embryonic ectoderm development protein (EED), and induces trimethylation of histone H3 at Lysine 27 (H3K27me3), contributes to the formation of a repressive chromatin state and transient transcriptional inhibition at sites of oxidative DNA damage (O'Hagan et al. 2011). DNA methyltransferase 1 (DNMT1) methylates newly synthesized DNA during DNA replication and participates in maintaining epigenetic silencing of key genes implicated in human cancers (Robert et al. 2003).

The recruitment of DNA repair and epigenetic silencing proteins to promoter CpG islands in response to ROS may be important for initiating aberrant DNA methylation. Guanine residues in DNA are a primary target for ROS during inflammation, with 8-oxo-G being the most abundant form of oxidative damage

(Ba et al. 2014). Due to high guanine content, promoter CpG islands are hotspots for 8-oxo-G and therefore oxidative DNA damage. 8-oxo-G lesions are repaired by base excision repair (David et al. 2007) and non-canonical MMR (Zlatanou et al. 2011) pathways. We have shown that MMR proteins MSH2 and MSH6 have an increase in affinity for chromatin after 30 min of H_2O_2 treatment (Ding et al. 2016). MSH2 and MSH6 recruit epigenetic silencing proteins DNMT1 and EZH2 to sites of oxidative damage through a protein-protein interaction-dependent mechanism (Ding et al. 2016). *In vitro* and *in vivo*, we have demonstrated that the recruitment of DNMT1 and EZH2 to sites of oxidative DNA damage results in increased H3K27me3 deposition in the promoters of candidate TSGs that is associated with decreased gene expression (O'Hagan et al. 2011; Maiuri et al. 2017). *In vivo*, this early recruitment to sites of oxidative damage results in sustained DNA hypermethylation of the TSGs' promoter CpG islands in tumors that form as a result of chronic inflammation (Maiuri et al. 2017). These findings are congruent with the knowledge that cancer-specific aberrant gains in DNA methylation tend to occur at gene promoters enriched for H3K27me3 (Schlesinger et al. 2007; Rose and Klose 2014). However, the upstream mechanism for increased affinity of MSH2 and MSH6 for sites of oxidative DNA damage is still unclear.

The tyrosine kinase, Janus kinase 2 (JAK2), plays important roles during the inflammatory response (Boland et al. 2014), carcinogenesis (Du et al. 2012), DNA damage and repair (Gloc et al. 2002; Scott and Rebel 2012), and may regulate epigenetic alterations (Dawson et al. 2009). Canonical activation of JAK2 occurs in response to binding of various ligands such as interleukin-6 (IL-6) and growth hormones to the receptor to which JAK2 is bound. In this canonical response, activated JAK2 phosphorylates its downstream effector-Signal transducer and activator of transcription 3 (STAT3), which initiates transcription of genes associated with cell proliferation, differentiation and oncogenesis (Wang and Sun 2014). In contrast, ROS induces JAK2 signaling activation in a ligand-independent fashion (Duan et al. 2013). In addition, ROS reduces STAT3 binding to its canonical binding targets such as consensus serum-inducible elements (SIE) and diminishes IL-6-mediated gene transcription (Li et al. 2010; Scott and Rebel

2012; Sobotta et al. 2015). These results suggest gene activation by the canonical JAK2 pathway and by the ROS-mediated pathway may be different. Mutant JAK2, which is constitutively active, also has non-canonical roles. Mutant JAK2 V617F can be localized in the nucleus, directly phosphorylate histone H3 at Y41, and regulate gene expression independently of ligand-activation or STAT3-interaction (Dawson et al. 2009).

Herein, we connect JAK2 to the MMR and epigenetic response to oxidative damage. We uniquely demonstrate that active wildtype JAK2 translocates to the nucleus in response to oxidative damage and that nuclear JAK2 plays a critical role in regulating MSH2, MSH6, DNMT1 and EZH2 chromatin binding, and global levels of H3K27me3. We further show that JAK2 is important for oxidative damage-induced transcriptional repression of candidate TSGs in colon cancer cells. Understanding the connection between JAK2, MSH2, MSH6, and epigenetic alterations will provide key insight into how aberrant epigenetic alterations are initiated during chronic inflammation.

Materials and methods

Cell culture and treatments

NCCIT and SW480 cells were purchased from American Tissue Type Culture Collection (ATCC) and maintained in RPMI 1640 and McCoy's 5A media (Corning, PA), respectively with 10% fetal bovine serum (Gibco, MA). H_2O_2 treatment was performed as previously described (Ding et al. 2016). Tyrphostin AG490 (Sigma, MO, T3434-5MG) was dissolved in DMSO (Sigma, MO) and further diluted before adding it to the media. Cells were treated with 100 μM Tyrphostin AG490 for 6 hours prior to H_2O_2 exposure. BMS-911543 (Biovision, CA, 2630-5) was dissolved in DMSO (Sigma, MO) and further diluted before adding it to the media. Cells were treated with 2.2 nM BMS-911543 for 6 hours prior to H_2O_2 exposure.

shRNA knockdown

For shRNA knockdown of JAK2 and Non-target (NT), cells were infected with lentiviral particles for 96 hours with puromycin (Sigma, MO) selection before collection following the manufacturer's protocol (Sigma, MO). JAK2 (Sigma, MO, SHCLNG-NM_004972, TRCN000002181) and TRC2 (NT) (Sigma, MO, SHC201) were expressed using lentiviral particles following the lentiviral shRNA knockdown protocol from The RNAi Consortium Broad Institute.

Antibodies

For Co-IP of endogenous proteins, anti-JAK2 (Millipore, 06-255-I¸1:100), anti-MSH2 (Cell Signaling Technology (CST, MA), 2017S, 1:200), anti-MSH6 (Becton Dickinson (BD, NJ), 610918, 1:100), anti-EZH2 (CST, MA, 5246T, 1:200) antibodies were used. For western blot, anti-JAK2 (Millipore, 06-255-I, 1:1000 and Abcam, CA, ab108596, 1:1000), anti-p-JAK2 (Y1007/1008, 1:1000) (Millipore, MA, 07-606), anti-p-STAT3 (Y705) (CST, MA, 9145S, 1:1000), anti-LaminB (Santa Cruz (SC, CA), sc-6216, 1:1000), anti-GAPDH (CST, MA, 5174, 1:1000), anti-MSH2 (CST, MA, 2017S, 1:1000), anti-MSH6 (BD, 610918, 1:1000), anti-DNMT1 (Sigma, MO, D4692, 1:1000), anti-EZH2 (CST, MA, 3147S, 1:1000), anti-STAT3 (CST, MA, 9139, 1:1000), anti-γH2AX (CST, MA, 9718, 1:1000), anti-H3K27me3 (CST, MA, 9733, 1:1000), anti-H3 (CST, MA, 9751, 1:3000), anti-EZH2 (CST, MA, 3147S, 1:1000), anti-SUZ12 (CST, MA, 3737, 1:1000), anti-EED (Sigma, MO, GW10896A, 1:500) antibodies were used. For immunofluorescence, anti-JAK2 (Abcam, CA, ab108596, 1:100), anti-DNMT1 (SC, CA, sc-20701, 1:100), anti-γH2AX (Millipore, NJ, 05-636, 1:100), secondary Alexa Conjugate (CST, MA, mouse 8890, 1:500 and rabbit 8889, 1:1000) were used.

Nuclear/cytoplasmic extraction, chromatin affinity assay, and whole cell isolation

These assays were performed as previously described (Ding et al. 2016). Band densitometry for western blots were measured by Image J software (NIH). Band densitometry were first normalized to LaminB or H3 and then relative densitometry of proteins across treatments was normalized to the untreated condition.

Immunofluorescence and Co-IP

Immunofluorescence was performed with or without preextraction buffer as indicated. Immunofluorescence and Nuclear Co-IP were performed as previously described (Ding et al. 2016). Obtained fluorescence images were subjected to digital processing and background subtraction by Adobe Photoshop CS with identical conditions for each treatment group.

Histone methyltransferase activity assay (H3K27)

Nuclear extraction was performed followed by histone methyltransferase activity ELISA assay according to the manufacturer's protocol (EpiGenTEK, OP-0002-1 and P-3005-48).

qPCR (quantitative Polymerase Chain Reaction)

Total RNA was first isolated (Qiagen, 74104) and reverse transcribed according to the manufacturer's protocol (Thermo, K1642). cDNA was used for qPCR analysis with gene-specific primers and the reactions were detected using a FastStart Essential DNA Green Master (Roche, CA, 06402712001). The expression of mRNA was normalized to *glyceraldehyde 3-phosphate dehydrogenas*e (*GAPDH*) expression. (*GAPDH*; ΔCq = target mRNA *Cq* – GAPDH *Cq*). The individual primers used were listed below:

MLH1, forward, AAGCTCCTGGGCTCCAATTC

MLH1, reverse, CGAGGTCAGACTTGTTGTGGA

CDH1, forward, ATCCCACCACGTACAAGGGT

CDH1, reverse, GTGTATACAGCCTCCCACGC

GAPDH, forward, GAAGGTCGGAGTCAACGGATTT

GAPDH, reverse, ATGGGTGGAATCATATTGGAC

Statistical analysis

Relative densitometry, cell foci and qPCR data are presented as the mean ± standard error (SEM). These data are evaluated by one-way ANOVA with multiple comparisons and considered statistically significant with a *p*-value < 0.05. The number of replicates for each experiment is included in figure legends.

Results

Oxidative damage induces catalytic activity-dependent JAK2 nuclear translocation.

In the canonical JAK2-STAT3 pathway, JAK2 becomes active, is autophosphorylated (p-JAK2 at Y1007/1008) and recruits STAT3 for phosphorylation (p-STAT3) in response to IL-6 stimulation (Wang and Sun 2014). While p-STAT3 translocates to the nucleus upon IL-6 treatment, activated JAK2 is retained in the cytoplasm by remaining bound to its receptor. To test if H_2O_2 changes the subcellular localization of endogenous JAK2, nuclear and cytoplasmic fractions were isolated from untreated or treated human embryonic carcinoma (NCCIT) cells. In contrast to IL-6, H_2O_2 treatment increases JAK2 protein levels in the nuclear fraction and decreases levels in the cytoplasmic fraction, as compared to untreated cells (Figure 1A). To confirm these results, experiments were repeated with a different JAK2 antibody. We demonstrated that both antibodies detect a band at the molecular weight of 131 kDa in whole cell extracts from non-target knockdown (NT) NCCIT cells and this band is reduced in JAK2 knockdown cells with or without H_2O_2 treatment, confirming the specificity of the two JAK2 antibodies (Supplementary Figure 1A). To determine if JAK2 catalytic activity is important for JAK2 nuclear translocation, cells were treated with the JAK2 inhibitor Tyrphostin AG490 6 hours prior to H_2O_2 treatment and nuclear extractions were performed. Inhibiting JAK2 activity significantly reduces JAK2 and p-JAK2 nuclear localization (Figure 1B). In confirmation of the efficacy of the inhibitor, AG490 treatment reduces IL-6-induced levels of p-STAT3 (Figure 1B). Although Tyrphostin AG490 is a potent JAK2 inhibitor, it also nonspecifically inhibits other protein tyrosine kinases (Sayyah and Sayeski 2009). Therefore, we used BMS-911543, a highly selective JAK2 inhibitor, to further validate our findings. At a nanomolar concentration BMS-911543 only inhibits the activity of JAK2 but not JAK1, JAK3 or SET-2 (Wan et al. 2015). Inhibition of JAK2 by pretreatment with 2.2 nM BMS-911543 also reduces the H_2O_2-

induced nuclear localization of JAK2 (Figure 1C). To further confirm JAK2 nuclear translocation, JAK2 subcellular localization was assessed by immunofluorescence. Low levels of JAK2 are present throughout the cell in untreated cells and cells treated with IL-6, whereas nuclear staining is detected after H_2O_2 treatment (Figure 1D). Knockdown of JAK2 reduces oxidative damage-induced JAK2 signal in nuclei, suggesting this nuclear signal is JAK2 specific (Supplementary Figure 1B). In confirmation of our western blot findings, inhibiting JAK2 catalytic activity with Tyrphostin AG490 abrogates the oxidative damage-induced nuclear localization of JAK2, suggesting JAK2 nuclear localization in response to oxidative damage is dependent on its catalytic activity.

Inhibition of JAK2 alters oxidative damage-induced chromatin binding of MSH6, MSH2 and DNMT1

Previously, it was demonstrated that MSH2 and MSH6 are predominantly localized in the cytoplasm basally but translocate into the nucleus and interact with DNMT1 in response to oxidative damage (Ding et al. 2016). Since we observed that oxidative damage also induces JAK2 nuclear translocation (Figure 1A), we initially hypothesized that nuclear localization of MSH2 and MSH6 after oxidative damage may be dependent on JAK2. However, as demonstrated by protein levels in nuclear fractions (Supplementary Figure 2A) from BMS911543 or Tyrphostin AG490 treated cells and nuclear inputs used for co-immunoprecipitation (co-IP) after Tyrphostin AG490 treatment (Supplementary Figure 3A and 3B), JAK2 inhibition does not affect nuclear levels of MSH2, MSH6 or DNMT1 basally or in response to oxidative damage. By using a chromatin affinity assay that includes a high concentration salt buffer wash, we previously demonstrated that oxidative damage increases the affinity of MSH2, MSH6 and DNMT1 for chromatin (Ding et al. 2016). In response to H_2O_2 treatment, JAK2 also has increased affinity for chromatin (Figure 2A). Importantly, inhibition of JAK2 by Tyrphostin AG490 reduces the H_2O_2-induced increase in affinity of MSH6, DNMT1 and JAK2 for chromatin. JAK2 inhibition prevents a statistically significant increase in affinity of MSH2 for chromatin after H_2O_2 treatment when comparing untreated and H_2O_2-treated JAK2-inhibited samples. However, JAK2 inhibition does not significantly reduce the

increase in affinity of MSH2 for chromatin in response to H_2O_2 treatment as compared with H_2O_2 treatment alone (Figure 2A). This finding suggests that there may be an additional mechanism for H_2O_2-induced MSH2 chromatin binding, possibly through its interaction with MSH3 as part of MutSβ, which we have demonstrated occurs basally and after oxidative damage (Ding et al. 2016). The total cellular levels of MSH2, MSH6 and DNMT1 are not affected by Tyrphostin AG490 or H_2O_2 treatment (Figure 2A). Moreover, inhibition of JAK2 by Tyrphostin AG490 increases the level of γH2AX basally and after oxidative damage (Figure 2A), consistent with a previous report that JAK2 activation causes an increase in homologous recombination (Gloc et al. 2002). Consistent with the effect of Tyrphostin AG490, inhibition of JAK2 by BMS-911543 reduces the H_2O_2-induced increase in affinity of MSH6, MSH2, DNMT1 and JAK2 for chromatin (Figure 2B). BMS-911543 treatment reduces oxidative damage-induced levels of p-STAT3 (Figure 2B), confirming the efficacy of the inhibitor. There is a trend for an increase of γH2AX levels in response to BMS911543 treatment basally and after oxidative damage, but this change is not significant (Figure 2B). To confirm these findings, binding of MSH2, MSH6 and DNMT1 to chromatin following knockdown of JAK2 by lentiviral shRNA was analyzed. Knockdown of JAK2 reduces oxidative damage-induced chromatin binding of MSH6 and DNMT1 without affecting total protein levels of MSH6 or DNMT1 (Figure 2C). Again, there is a trend for reduction in affinity for MSH2, but this change is not significant (Figure 2C). Consistent with our previous results (Ding et al. 2016), knockdown of MSH6 reduces oxidative damage-induced chromatin interaction of MSH6 and DNMT1 but does not affect total protein level of DNMT1 (Figure 2C).

Immunofluorescence can also be used to interrogate DNMT1's response to oxidative damage because oxidative damage induces DNMT1 foci that co-localize with the DNA damage marker γH2AX (Ding et al. 2016) (Supplementary Figure 2B). Inhibition or knockdown of JAK2 abrogates the formation of oxidative damage-induced DNMT1 foci and the co-localization between DNMT1 and γH2AX (Supplementary Figure 2B and 2C). Consistent with the western blot results (Figure 2A and 2B),

inhibition or knockdown of JAK2 elevates levels of γH2AX basally and after oxidative damage in immunofluorescence analysis (Supplementary Figure 2B and 2C).

Besides JAK2 oxidative damage also activates several other protein kinases such as Protein kinase C (PKC), Protein kinase B (PKB or AKT), Jun N-terminal kinases (JNK), mitogen-activated protein kinase (MAPK) (Martindale and Holbrook 2002). Treatment of cells with inhibitors of these kinases (Staurosporine (PKCi), LY294002 (PI3K/AKTi), SP600125 (JNKi), SB203580 (MAPKi)) at doses that reduce known downstream targets does not reduce oxidative damage-induced MSH2, MSH6 or DNMT1 chromatin binding (data not shown), suggesting these protein kinases do not regulate the chromatin binding of MSH2, MSH6 and DNMT1 in response to oxidative damage.

JAK2 interacts with MSH2 and MSH6 in the nucleus in response to H_2O_2 treatment

In response to H_2O_2 treatment, MSH6, MSH2, DNMT1 and JAK2 concordantly have increased affinity for chromatin (Figure 2A). We hypothesized that nuclear JAK2 interacts with one or multiple of these proteins and therefore cytoplasmic and nuclear Co-IPs were performed to study the protein-protein interactions in different cellular compartments. Previously we have demonstrated that MSH2 and MSH6 primarily localize in the cytoplasm in the basal state in NCCIT cells (Ding et al. 2016). Here, we demonstrate that MSH2 interacts with JAK2 and MSH6 in the untreated state in the cytoplasm (Figure 3A). In response to oxidative damage, the interaction of MSH2 with MSH6 in the cytoplasm is reduced and there is no detectable JAK2 in the cytoplasm. (Figure 3A). In response to H_2O_2 treatment, levels of MSH2, MSH6 and JAK2 in the nuclear input fraction are increased consistent with their nuclear translocation (Figure 3B-3D); whereas DNMT1and EZH2 are unchanged. JAK2 interacts with MSH2 and MSH6 in nuclear fractions in response to H_2O_2, while no interaction is detected in untreated cells (Figure 3B). No interaction is detected between nuclear JAK2 and epigenetic proteins, including DNMT1, EZH2, SUZ12 or EED2 basally or in response to H_2O_2 (Figure 3B and data not shown). Nuclear Co-IPs using antibodies against MSH2 and MSH6 confirm their interaction with JAK2 in the nucleus after H_2O_2

treatment (Figure 3C and 3D). Together, these findings demonstrate that MSH2 interacts with JAK2 basally in the cytoplasm and oxidative damage induces the nuclear translocation of MSH2, MSH6 and JAK2 resulting in their interaction in the nucleus.

Inhibition of JAK2 alters the PRC2 response to oxidative damage.

Previously, we have demonstrated that oxidative damage induces the DNMT1-dependent interaction of MSH2 and MSH6 with PRC2 members, EZH2, SUZ12, and EED2 (O'Hagan et al. 2011) (Ding et al. 2016). Because inhibition of JAK2 alters the interaction of DNMT1 with chromatin, it may also affect the chromatin affinity of PRC2 members. Interestingly, although H_2O_2 alone does not increase the affinity of EZH2 and EED for chromatin, inhibition of JAK2 by Tyrphostin AG490 or BMS-911543 significantly reduces EZH2 and EED2 chromatin affinity after H_2O_2 treatment (Figure 4A and 4B). After H_2O_2 treatment, there is a trend for reduction in affinity for SUZ12 with inhibition of JAK2 by either Tyrphostin AG490 or BMS-911543, but the effect of Tyrphostin AG490 is not significant (Figure 4A and 4B). These results were further validated in the SW480 colon cancer cell line (Supplementary Figure 4A). To test if JAK2 alters the protein-protein interactions between MSH6, DNMT1 and PRC2, nuclear Co-IPs were performed using antibodies against MSH6 or EZH2 in cells where JAK2 was inhibited followed by 30 min H_2O_2 treatment. JAK2 inhibition does not alter the oxidative damage-induced interaction of MSH6, DNMT1, and PRC2 (Supplementary Figure 3A and 3B).

The finding that JAK2 alters the chromatin interaction of PRC2 members in response to oxidative damage suggests a potential functional role for JAK2 in regulating the level of H3K27me3 after oxidative damage. As previously demonstrated, 3 hours after H_2O_2 treatment, there is a global increase of H3K27me3 (Niu et al. 2015). Knockdown of JAK2 significantly reduces oxidative damage-induced H3K27me3 levels (Figure 4C). H_2O_2 can alter the catalytic activity of enzymes (Rhee et al. 2000) and EZH2's activity can be altered by post-translational modifications (Karantanos and Boussiotis 2016).

However, neither JAK2 knockdown nor H_2O_2 treatment alters the H3K27me3 histone methyltransferase activity in cellular lysates compared to basal NT cells (Supplementary Figure 4B).

Oxidative damage causes a transient reduction in transcription of CpG island containing genes, including the TSGs *CDH1* (Cadherin1 or E-cadherin) and *MLH1* (MutL homolog 1) that commonly undergo gene silencing and promoter CpG island hypermethylation in colorectal cancer (Wheeler et al. 2001; Li et al. 2013). This reduction in transcription is dependent on the MSH2/6-mediated recruitment of epigenetic proteins to chromatin (Ding et al. 2016). Consistent with these results, H_2O_2 treatment leads to a reduction in gene expression of *CDH1* and *MLH1* in SW480 cells and JAK2 inhibition significantly abrogates this reduction in transcription (Figure 4D). Altogether, these findings suggest that JAK2 regulates oxidative damage-induced global changes in H3K27me3 and transcription of candidate TSGs through altering the interaction of MSH2/MSH6, DNMT1 and PRC2 member proteins with chromatin.

JAK2 expression is associated with CIMP in human colorectal cancer.

Cancer-specific aberrant gains in DNA methylation tend to occur at gene promoters enriched for H3K27me3 (Schlesinger et al. 2007; Rose and Klose 2014). In humans, tumors bearing a high frequency of occurrence of aberrant promoter CpG island DNA hypermethylation are defined as CIMP-high (CIMP-H), whereas tumors bearing lower frequency or minimal CpG island hypermethylation are referred to as CIMP-L or non-CIMP, respectively. CIMP positive status is associated with poor prognosis and worse treatment outcome than non-CIMP status in colorectal cancer patients (Van Rijnsoever et al. 2003). Having demonstrated JAK2 is important for the recruitment of DNMT1 to sites of damage and global induction of H3K27me3, we next examined if JAK2 is associated with aberrant DNA hypermethylation in colorectal cancer, using CIMP status as a surrogate marker for promoter CpG island hypermethylation. In JAK2 RNA-seq data and CIMP status obtained from the TCGA colorectal cancer database (The Cancer Genome Atlas, COADREAD) (The Cancer Genome Atlas Network 2012), CIMP-H status correlates with higher expression of JAK2 mRNA, whereas CIMP-L or non-CIMP (Cluster 3 and 4)

cancers have lower gene expression of JAK2 (Figure 5), suggesting JAK2 expression is closely associated with promoter CpG island methylation in colorectal cancer.

Discussion

Recent studies demonstrate that kinases activated by cellular stress can alter the function of epigenetic proteins, leading to increased epigenetic regulation in cells (Cha et al. 2005; Kim et al. 2013). In the present study, we link the oxidative damage-induced activation and nuclear localization of JAK2 to the enrichment of MMR and epigenetic silencing proteins on damaged chromatin. This response is associated with changes in global levels of H3K27me3, and transcriptional repression of candidate TSGs in cancer. Furthermore, JAK2 mRNA expression is closely associated with CIMP-H status in colorectal cancer. While it is well known that constitutive activation of JAK2 can induce neoplastic transformation and cancer progression by activating downstream STAT proteins and promoting oncogenic transcription in hematopoietic malignancies (Vainchenker et al. 2008), much less is known regarding non-canonical roles of nuclear JAK2 in solid tumors. The role of JAK2 activity and non-canonical nuclear localization in the MMR and epigenetic responses to oxidative damage potentially links JAK2 to tumor progression in a novel way.

JAK2 is canonically studied as a cytoplasmic protein that is bound to a receptor and transmits information in response to ligand binding to the receptor to effect downstream gene transcription. In this study, we identified a noncanonical role of JAK2 in response to oxidative damage in human cells that is uncoupled from its role in the classic, ligand-dependent pathway. We demonstrate that in response to oxidative damage, JAK2 can localize to the nucleus, while activation of JAK2 in a canonical manner by IL-6 treatment does not induce such a change. This finding indicates that oxidative damage may employ different mechanisms from IL-6 to activate JAK2, possibly through oxidizing and inhibiting JAK2's negative regulator-protein tyrosine phosphatases (PTPs), including Cluster of differentiation 45 (CD45) and Src homology region 2 domain-containing phosphatase-1 (SHP1) (Oh et al. 2009). JAK2 is basally

inhibited and dephosphorylated at Y1007/1008 by PTPs (Li et al. 2015). ROS induce thiol oxidation in the catalytic sites of PTPs and this modification permits release of JAK2 from the PTPs, resulting in activation of JAK2 (Knobler and Elson 2014) (Oh et al. 2009). In line with these findings, we connect JAK2 nuclear translocation to its activity by demonstrating that inhibition of JAK2 induces dephosphorylation of JAK2 at Y1007/1008 and reduces oxidative damage-induced nuclear localization of JAK2. Further supporting the role of JAK2 phosphorylation in mediating JAK2 nuclear translocation, the JAK2 kinase-dead mutant K882E shows basally low nuclear localization signal, whereas the constitutively active JAK2 V617F has high nuclear localization signal (Sedek and Strous 2013).

Epigenetic proteins are involved in the DNA damage response and it is hypothesized that DNA repair pathways recruit epigenetic proteins to assist in the DNA repair process. The role of epigenetic proteins in DNA repair has been described by the "access-repair-restore" model (Green and Almouzni 2002; Ding et al. 2017). In response to damage, "active" chromatin modifiers such as histone acetyltransferases (HATs) and chromatin remodeling complexes are first recruited to the sites of DNA damage to "open" local chromatin structure allowing DNA repair proteins to gain access. Once DNA repair proteins access DNA, "repressive" chromatin modifiers such as histone deacetylases (HDACs) are recruited to "close" the chromatin and repress transcriptional activity. Finally, chromatin is restored back to its original state when repair is completed (Ding et al. 2017). In response to oxidative DNA damage, we demonstrated that (1) JAK2 is recruited to chromatin, (2) JAK2 interacts with MSH2 and MSH6 in the nucleus, and (3) inhibiting JAK2 alters the chromatin interaction of MSH2, MSH6, DNMT1, and PRC2 members. JAK2 inhibition or knockdown does not alter oxidative damage-induced nuclear localization of MSH2 and MSH6 suggesting that the increased chromatin association of MSH2 and MSH6 in response to oxidative damage is not through their increased nuclear localization. Based on these results, we hypothesize that in response to oxidative damage, JAK2 recruits MSH2 and MSH6 to promoter CpG islands that contain clustered oxidative damage as a result of preferential oxidative damage of guanines. Previous studies demonstrated that constitutively active mutant JAK2 acts as an "active" chromatin modifier, which can

directly interact and phosphorylate histone H3 at Y41 (H3Y41ph) to promote downstream transcription (Dawson et al. 2009). The H3Y41ph mark is associated with transcriptional activity and is primarily present at promoter transcription start sites (TSS) of active genes. Importantly, inhibition of JAK2 significantly reduces H3Y41ph at the TSS of genes (Dawson et al. 2012). We hypothesize that in response to oxidative damage, JAK2 is recruited to chromatin to mediate chromatin-based changes at damaged promoters and these changes facilitate DNA repair. The association of JAK2 with active chromatin may first open up local chromatin structure to allow MSH2 and MSH6 to gain access to clustered oxidative DNA damage. After accessing the damage, MSH2 and MSH6 recruit "repressive" epigenetic proteins including DNMT1 and PRC2 members to sites of damage. This recruitment results in a transient reduction in transcription so that transcription does not interfere with the DNA repair (Ding et al 2016). An alternative hypothesis is that JAK2 may regulate the chromatin interaction of MSH2 and MSH6 through phosphorylation of MSH2 and/or MSH6. There are known phosphorylation events that alter the MMR response to DNA damage. For example, MSH2 can be phosphorylated by the tyrosine kinase NPM-ALK in a manner that inhibits dimerization of MSH2 with MSH6 (Bone et al. 2015). We immunoprecipitated MSH2 and MSH6 from nuclear extracts from both untreated and H_2O_2 treated NCCIT cells and performed LC-MS/MS tandem mass spectrometry in an effort to identify tyrosine phosphorylation modifications on MSH2 and MSH6, but were unable to detect these modifications. Because of the known difficulty in detecting tyrosine phosphorylation on large proteins by mass spectrometry, we cannot rule out the possibility that JAK2's regulation of MSH2 and MSH6 is through a phosphorylation event. Further studies on how JAK2 increases the affinity of MSH2 and MSH6 for chromatin in response to oxidative damage are needed.

Our findings suggest one potential mechanism for the initiation of abnormal silencing of TSGs during tumorigenesis. We provide a novel link between JAK2, recruitment of repressive proteins and transient loss of gene expression in response to oxidative damage. JAK2 signaling is well known for its function upstream of transcriptional activation of genes that are responsible for growth and proliferation. However,

the findings presented here uniquely suggest that oxidative damage-induced nuclear JAK2 regulates chromatin enrichment of DNA repair proteins, epigenetic silencing proteins, and H3K27me3, thereby facilitating repression of candidate TSGs. JAK2 may also be linked to aberrant promoter CpG island DNA hypermethylation seen in human cancers. The JAK2-dependency of enhanced binding of DNMT1 to chromatin in response to oxidative damage, suggests that JAK2 is important for aberrant DNMT1 targeting during DNA damage. Recruitment of DNMT1 to sites of damage can result in sustained, aberrant DNA methylation of gene promoters both *in vitro* and *in vivo* (O'Hagan et al. 2008) (Maiuri et al. 2017). In line with these results, we demonstrate that JAK2 mRNA expression is associated with CIMP status in colorectal cancer. Together these results suggest JAK2 may participate in the initiation of aberrant DNA methylation during chronic inflammation.

Epigenetic therapy such as treatment with DNMT inhibitors azacytidine and decitabine is currently recommended to treat high risk myelodysplastic syndromes (MDS) and acute myeloid leukemia (AML). DNMT inhibitors are also currently being used to treat solid tumors in clinical trials. Despite their promising clinical future, success of these agents may depend on the durability of the DNA demethylation induced by them (Kagey et al. 2010). Azacytidine treatment of cells in vitro effectively reverses DNA hypermethylation. However, after removing azacytidine from the cells, genes reaccumulate promoter DNA hypermethylation over time (McGarvey et al. 2006). This result is possibly due to the fact that azacytidine only alters DNA methylation but does not alter the low levels of repressive chromatin marks, including H3K27me3 that are present at these promoters (McGarvey et al. 2006). This may be critical, as retention of H3K27me3 is known to recruit DNMTs and induce DNA methylation (McGarvey et al. 2006). Inhibition of JAK2 by Tyrphostin AG490 or BMS-911543 results in reduced binding of DNMT1 and PRC2 members to chromatin, which may result in reduction of H3K27me3 deposition on genes during inflammation and carcinogenesis and reduce their resilencing after azacytidine treatment is stopped. However, whether JAK2 inhibition affects re-silencing of aberrantly DNA hypermethylated genes requires further study and validation. In addition, inhibiting JAK2 by BMS-911543 is shown to be

safe, well tolerated in human, and this inhibitor is currently in clinical trials for treatment of myelofibrosis (Roberts et al. 2013). While further studies are required, nuclear JAK2 may be a potential target for the development of additional therapeutics for inflammation-driven cancers.

In summary, we demonstrate that in response to oxidative damage, JAK2 is activated and translocates into the nucleus where it plays a key role in regulating MSH2 and MSH6 binding to damaged chromatin. Through its regulation of MSH2 and MSH6, JAK2 also affects oxidative-damage induced increases in DNMT1 and EZH2 chromatin affinity, chromatin modifications and changes in gene expression of candidate TSGs. Furthermore, we demonstrate that JAK2 mRNA expression is closely correlated with CIMP status in human colorectal cancer.

Statement of Author Contributions

ND performed the majority of the cell and molecular biology work. SAM provided assistance with bioinformatics analysis and study design. SSS performed and analyzed some experiments. HMOH contributed to study concept and supervised ND's approach to data analysis. ND performed statistical analysis and generated text of manuscript. ND, SAM and HMOH critically revised the manuscript. All authors read and approved the final manuscript.

Acknowledgments

We thank the Indiana University Light Microscopy Imaging Center and Indiana University Center for Genomics and Bioinformatics for their assistance. This work was supported by the National Institute of Environmental Health Sciences Grant [R01ES023183 to HMOH]; and the National Institutes of Health, National Center for Advancing Translational Sciences, Clinical and Translational Sciences Award [TL1 TR001107 and UL1 TR001108 (A. Shekhar, PI) to SAM]

Conflict of Interest Declaration

None declared.

References

Ba X, Aguilera-Aguirre L, Rashid QTAN, Bacsi A, Radak Z, Sur S, Hosoki K, Hegde ML, Boldogh I. 2014. The role of 8-oxoguanine DNA glycosylase-1 in inflammation. International journal of molecular sciences 15(9):16975-16997.

Bannister AJ, Kouzarides T. 2011. Regulation of chromatin by histone modifications. Cell research 21(3):381.

Boland BS, Sandborn WJ, Chang JT. 2014. Update on Janus kinase antagonists in inflammatory bowel disease. Gastroenterol Clin North Am 43(3):603-617.

Bone KM, Wang P, Wu F, Wu C, Li L, Bacani JT, Andrew SE, Lai R. 2015. NPM-ALK mediates phosphorylation of MSH2 at tyrosine 238, creating a functional deficiency in MSH2 and the loss of mismatch repair. Blood Cancer J 5:e311.

Cha T-L, Zhou BP, Xia W, Wu Y, Yang C-C, Chen C-T, Ping B, Otte AP, Hung M-C. 2005. Akt-mediated phosphorylation of EZH2 suppresses methylation of lysine 27 in histone H3. science 310(5746):306-310.

David SS, O'shea VL, Kundu S. 2007. Base-excision repair of oxidative DNA damage. Nature 447(7147):941.

Dawson MA, Bannister AJ, Gottgens B, Foster SD, Bartke T, Green AR, Kouzarides T. 2009. JAK2 phosphorylates histone H3Y41 and excludes HP1alpha from chromatin. Nature 461(7265):819-822.

Dawson MA, Foster SD, Bannister AJ, Robson SC, Hannah R, Wang X, Xhemalce B, Wood AD, Green AR, Gottgens B, Kouzarides T. 2012. Three distinct patterns of histone H3Y41 phosphorylation mark active genes. Cell Rep 2(3):470-477.

Ding N, Bonham EM, Hannon BE, Amick TR, Baylin SB, O'hagan HM. 2016. Mismatch repair proteins recruit DNA methyltransferase 1 to sites of oxidative DNA damage. Journal of molecular cell biology 8(3):244-254.

Ding N, Maiuri AR, O'Hagan HM. 2017. The Emerging Role of Epigenetic Modifiers in Repair of DNA Damage Associated with Chronic Inflammatory Diseases. Mutation Research/Reviews in Mutation Research.

Du W, Hong J, Wang YC, Zhang YJ, Wang P, Su WY, Lin YW, Lu R, Zou WP, Xiong H, Fang JY. 2012. Inhibition of JAK2/STAT3 signalling induces colorectal cancer cell apoptosis via mitochondrial pathway. J Cell Mol Med 16(8):1878-1888.

Duan W, Yang Y, Yi W, Yan J, Liang Z, Wang N, Li Y, Chen W, Yu S, Jin Z. 2013. New role of JAK2/STAT3 signaling in endothelial cell oxidative stress injury and protective effect of melatonin. PloS one 8(3):e57941.

Gloc E, Warszawski M, Mlynarski W, Stolarska M, Hoser G, Skorski T, Blasiak J. 2002. TEL/JAK2 tyrosine kinase inhibits DNA repair in the presence of amifostine. Acta Biochim Pol 49(1):121-128.

Green CM, Almouzni G. 2002. When repair meets chromatin. First in series on chromatin dynamics. EMBO Rep 3(1):28-33.

Kagey JD, Kapoor-Vazirani P, McCabe MT, Powell DR, Vertino PM. 2010. Long-term stability of demethylation after transient exposure to 5-aza-2′-deoxycytidine correlates with sustained RNA polymerase II occupancy. Molecular Cancer Research 8(7):1048-1059.

Karantanos T, Boussiotis VA. 2016. JAK3-mediated phosphorylation of EZH2: a novel mechanism of non-canonical EZH2 activation and oncogenic function. Transl Cancer Res 5(Suppl 6):S1208-s1211.

Kim E, Kim M, Woo D-H, Shin Y, Shin J, Chang N, Oh YT, Kim H, Rheey J, Nakano I. 2013. Phosphorylation of EZH2 activates STAT3 signaling via STAT3 methylation and promotes tumorigenicity of glioblastoma stem-like cells. Cancer cell 23(6):839-852.
Knobler H, Elson A. 2014. Metabolic regulation by protein tyrosine phosphatases. J Biomed Res 28(3):157-168.
Kondo Y. 2009. Epigenetic cross-talk between DNA methylation and histone modifications in human cancers. Yonsei medical journal 50(4):455-463.
Li J, Liu X, Chu H, Fu X, Li T, Hu L, Xing S, Li G, Gu J, Zhao ZJ. 2015. Specific dephosphorylation of Janus Kinase 2 by protein tyrosine phosphatases. Proteomics 15(1):68-76.
Li L, Cheung S-h, Evans EL, Shaw PE. 2010. Modulation of gene expression and tumor cell growth by redox modification of STAT3. Cancer research 70(20):8222-8232.
Li X, Yao X, Wang Y, Hu F, Wang F, Jiang L, Liu Y, Wang D, Sun G, Zhao Y. 2013. MLH1 promoter methylation frequency in colorectal cancer patients and related clinicopathological and molecular features. PLoS One 8(3):e59064.
Maiuri AR, Peng M, Sriramkumar S, Kamplain CM, Shields CD, Sears CL, O'Hagan HM. 2017. Mismatch repair proteins initiate epigenetic alterations during inflammation-driven tumorigenesis. Cancer research:canres. 0056.2017.
Martindale JL, Holbrook NJ. 2002. Cellular response to oxidative stress: signaling for suicide and survival. J Cell Physiol 192(1):1-15.
McGarvey KM, Fahrner JA, Greene E, Martens J, Jenuwein T, Baylin SB. 2006. Silenced tumor suppressor genes reactivated by DNA demethylation do not return to a fully euchromatic chromatin state. Cancer Res 66(7):3541-3549.
The Cancer Genome Atlas Network 2012. Comprehensive molecular characterization of human colon and rectal cancer. Nature 487(7407):330.
Niu Y, DesMarais TL, Tong Z, Yao Y, Costa M. 2015. Oxidative stress alters global histone modification and DNA methylation. Free Radic Biol Med 82:22-28.
O'Hagan HM, Mohammad HP, Baylin SB. 2008. Double strand breaks can initiate gene silencing and SIRT1-dependent onset of DNA methylation in an exogenous promoter CpG island. PLoS Genet 4(8):e1000155.
O'Hagan HM, Wang W, Sen S, Destefano Shields C, Lee SS, Zhang YW, Clements EG, Cai Y, Van Neste L, Easwaran H, Casero RA, Sears CL, Baylin SB. 2011. Oxidative damage targets complexes containing DNA methyltransferases, SIRT1, and polycomb members to promoter CpG Islands. Cancer Cell 20(5):606-619.
Oh J, Hur MW, Lee CE. 2009. SOCS1 protects protein tyrosine phosphatases by thioredoxin upregulation and attenuates Jaks to suppress ROS-mediated apoptosis. Oncogene 28(35):3145-3156.
Rhee SG, Bae YS, Lee SR, Kwon J. 2000. Hydrogen peroxide: a key messenger that modulates protein phosphorylation through cysteine oxidation. Sci STKE 2000(53):pe1.
Robert MF, Morin S, Beaulieu N, Gauthier F, Chute IC, Barsalou A, MacLeod AR. 2003. DNMT1 is required to maintain CpG methylation and aberrant gene silencing in human cancer cells. Nat Genet 33(1):61-65.
Roberts AW, Seymour JF, Burbury K, Verstovsek S, Kantarjian HM, Begna K, Yoshitsugu H, Gestone TA, Phillips P, Xing G. 2013. BMS-911543, a selective JAK2 inhibitor: a multicenter phase 1/2a study in myelofibrosis. Am Soc Hematology.
Rose NR, Klose RJ. 2014. Understanding the relationship between DNA methylation and histone lysine methylation. Biochimica et Biophysica Acta (BBA)-Gene Regulatory Mechanisms 1839(12):1362-1372.
Sayyah J, Sayeski PP. 2009. Jak2 inhibitors: rationale and role as therapeutic agents in hematologic malignancies. Current oncology reports 11(2):117-124.

Schlesinger Y, Straussman R, Keshet I, Farkash S, Hecht M, Zimmerman J, Eden E, Yakhini Z, Ben-Shushan E, Reubinoff BE. 2007. Polycomb-mediated methylation on Lys27 of histone H3 pre-marks genes for de novo methylation in cancer. Nature genetics 39(2):232.

Scott LM, Rebel VI. 2012. JAK2 and genomic instability in the myeloproliferative neoplasms: a case of the chicken or the egg? Am J Hematol 87(11):1028-1036.

Sedek M, Strous GJ. 2013. SUMOylation is a regulator of the translocation of Jak2 between nucleus and cytosol. Biochemical Journal 453(2):231-239.

Sharma S, Kelly TK, Jones PA. 2010. Epigenetics in cancer. Carcinogenesis 31(1):27-36.

Sobotta MC, Liou W, Stöcker S, Talwar D, Oehler M, Ruppert T, Scharf AN, Dick TP. 2015. Peroxiredoxin-2 and STAT3 form a redox relay for H 2 O 2 signaling. Nature chemical biology 11(1):64.

Takeshima H, Wakabayashi M, Hattori N, Yamashita S, Ushijima T. 2015. Identification of coexistence of DNA methylation and H3K27me3 specifically in cancer cells as a promising target for epigenetic therapy. Carcinogenesis 36(2):192-201.

Vainchenker W, Dusa A, Constantinescu SN. JAKs in pathology: role of Janus kinases in hematopoietic malignancies and immunodeficiencies; 2008. Elsevier. p 385-393.

Van Rijnsoever M, Elsaleh H, Joseph D, McCaul K, Iacopetta B. 2003. CpG island methylator phenotype is an independent predictor of survival benefit from 5-fluorouracil in stage III colorectal cancer. Clin Cancer Res 9(8):2898-2903.

Wan H, Schroeder GM, Hart AC, Inghrim J, Grebinski J, Tokarski JS, Lorenzi MV, You D, Mcdevitt T, Penhallow B. 2015. Discovery of a highly selective JAK2 inhibitor, BMS-911543, for the treatment of myeloproliferative neoplasms. ACS medicinal chemistry letters 6(8):850-855.

Wang S-W, Sun Y-M. 2014. The IL-6/JAK/STAT3 pathway: potential therapeutic strategies in treating colorectal cancer. International journal of oncology 44(4):1032-1040.

Wheeler JM, Kim HC, Efstathiou JA, Ilyas M, Mortensen NJ, Bodmer WF. 2001. Hypermethylation of the promoter region of the E-cadherin gene (CDH1) in sporadic and ulcerative colitis associated colorectal cancer. Gut 48(3):367-371.

Zlatanou A, Despras E, Braz-Petta T, Boubakour-Azzouz I, Pouvelle C, Stewart GS, Nakajima S, Yasui A, Ishchenko AA, Kannouche PL. 2011. The hMsh2-hMsh6 complex acts in concert with monoubiquitinated PCNA and Pol η in response to oxidative DNA damage in human cells. Molecular cell 43(4):649-662.

Figure Legends

Figure 1. Oxidative damage induces catalytic activity-dependent JAK2 nuclear localization.

(A) Nuclear extractions were performed using NCCIT cells untreated or treated with 2 mM H_2O_2 for 30 min or IL-6 (10 ng/ml) for 10 min. LaminB and GAPDH are nuclear and cytoplasmic controls, respectively. The data presented are from one representative experiment of two biological replicates. (B) Nuclear extractions were performed using NCCIT cells untreated or treated with 100 μM Tyrphostin AG490 for 6 hours followed by 2 mM H_2O_2 for 30 min or 10 ng/ml IL-6 treatment for 10 min. p-STAT3 serves as a control for treatments. Relative densitometry data are displayed as mean±SEM for each

treatment condition for JAK2 and p-JAK2 (n = 3). **P < 0.01, "ns" indicates not significant, P > 0.05. (C) Nuclear fractions were prepared from NCCIT cells untreated or treated with 2.2 nM BMS-911543 for 6 hours followed by 30 min, 2 mM H_2O_2 treatment. Relative densitometry data are displayed as mean±SEM for each treatment condition (n = 3). *P < 0.05, "ns" indicates not significant, P > 0.05 (D) NCCIT cells were treated as in B followed by immunofluorescence analysis. Percentage of cells with nuclear JAK2 staining were quantified by counting five fields of view and displayed as mean ± SEM for each treatment condition (n = 3). **P < 0.01, "ns" indicates not significant, P > 0.05.

Figure 2. Inhibition of JAK2 alters oxidative damage-induced chromatin binding of MSH6 and DNMT1.

(A) Chromatin affinity assays were performed using NCCIT cells untreated or treated with 100 μM Tyrphostin AG490 for 6 hours followed by 30 min, 2 mM H_2O_2 treatment. Tight chromatin is the remaining protein in the chromatin pellet after extraction with 0.45 M NaCl buffer. Relative densitometry data are displayed as mean ± SEM for each treatment condition (n=3). *P < 0.05, **P < 0.01, "ns" indicates not significant, P > 0.05. (B) NCCIT cells were untreated or treated with 2.2 nM BMS-911543 for 6 hours followed by 30 min, 2 mM H_2O_2 treatment. Chromatin affinity assays and whole cell lysate extractions are performed. Relative densitometry data are displayed as mean±SEM for each treatment condition (n = 3). *P < 0.05, **P < 0.01, "ns" indicates not significant, P > 0.05. (C) NCCIT cells were infected with nontarget (NT), or JAK2 shRNA lentiviral particles. After 96 h, they were untreated or treated with 2 mM H_2O_2 for 30 min. Chromatin affinity assays and whole cell lysate extractions were performed. Relative densitometry data are displayed as mean ± SEM for each treatment condition (n = 3). *P < 0.05, **P < 0.01, "ns" indicates not significant, P > 0.05.

Figure 3. JAK2 interacts with MSH2 and MSH6 in the nucleus after oxidative damage.

(A) NCCIT cells were untreated (U) or treated (T) with 2 mM H_2O_2 for 30 min. Co-IPs from cytoplasmic cellular fractions were performed with control IgG or anti-MSH2 antibodies. (B) Cells were treated as in A and Co-IPs from nuclear fractions were performed with control IgG or anti-JAK2 antibodies (C) Cells were treated as in A and nuclear Co-IPs were performed with control IgG or anti-MSH2 antibodies. (D) Cells were treated as in A and Co-IPs were performed with control IgG and anti-MSH6 antibodies. All above data are from one representative experiment of two biological replicates.

Figure 4. Inhibiting JAK2 alters the PRC2 response to oxidative damage.

(A) Chromatin affinity assays were performed using NCCIT cells untreated or treated with 100 μM Tyrphostin AG490 for 6 hours followed by 30 min, 2 mM H_2O_2 treatment. * indicates EED2. Relative densitometry data are displayed as mean ± SEM for each treatment condition for EZH2, SUZ12 and EED2 (n = 3). *P < 0.05, "ns" indicates not significant, P > 0.05. ND indicates signal is not detected. (B) Chromatin affinity assays were performed using NCCIT cells untreated or treated with 2.2 nM BMS-911543 for 6 hours followed by 30 min, 2 mM H_2O_2 treatment. * indicates EED2. Relative densitometry data are displayed as mean ± SEM for each treatment condition for EZH2, SUZ12 and EED2 (n = 3). *P < 0.05, *P < 0.01, "ns" indicates not significant, P > 0.05. ND indicates signal is not detected. (C) Whole cell lysate was collected from NCCIT cells infected with nontarget (NT), or JAK2 shRNA lentiviral particles for 96 h followed by 3 hour, 0.25 mM H_2O_2 treatment. Relative densitometry data are displayed as mean±SEM for each treatment condition for H3K27me3 (n = 3). *P < 0.05, **P < 0.01, "ns" indicates not significant, P > 0.05. (D) SW480 cells were untreated or treated with 100 μM Tyrphostin AG490 for 6 hours followed by 3-hour, 0.5 mM H_2O_2 treatment. Total RNA was isolated and RT-qPCR is performed. Relative fold change displayed as mean ± SEM of H_2O_2 treated over untreated (n = 3). *P < 0.05, **P < 0.01.

Figure 5. JAK2 expression is associated with CIMP status in human colorectal cancer.

CIMP status and RNA-seq data were obtained from TCGA colorectal cancer database (COADREAD). One way ANOVA was used to test for statistical significance. The data are displayed as a box and whisker diagram showing 25th to 75th percentiles with the middle horizontal bar at the median. Whiskers are drawn using the Tukey method. (Cluster 3 and 4 are non-CIMP groups, RPKM indicates Reads Per Kilo base per Million.) $^{**}P < 0.01$.

Figures

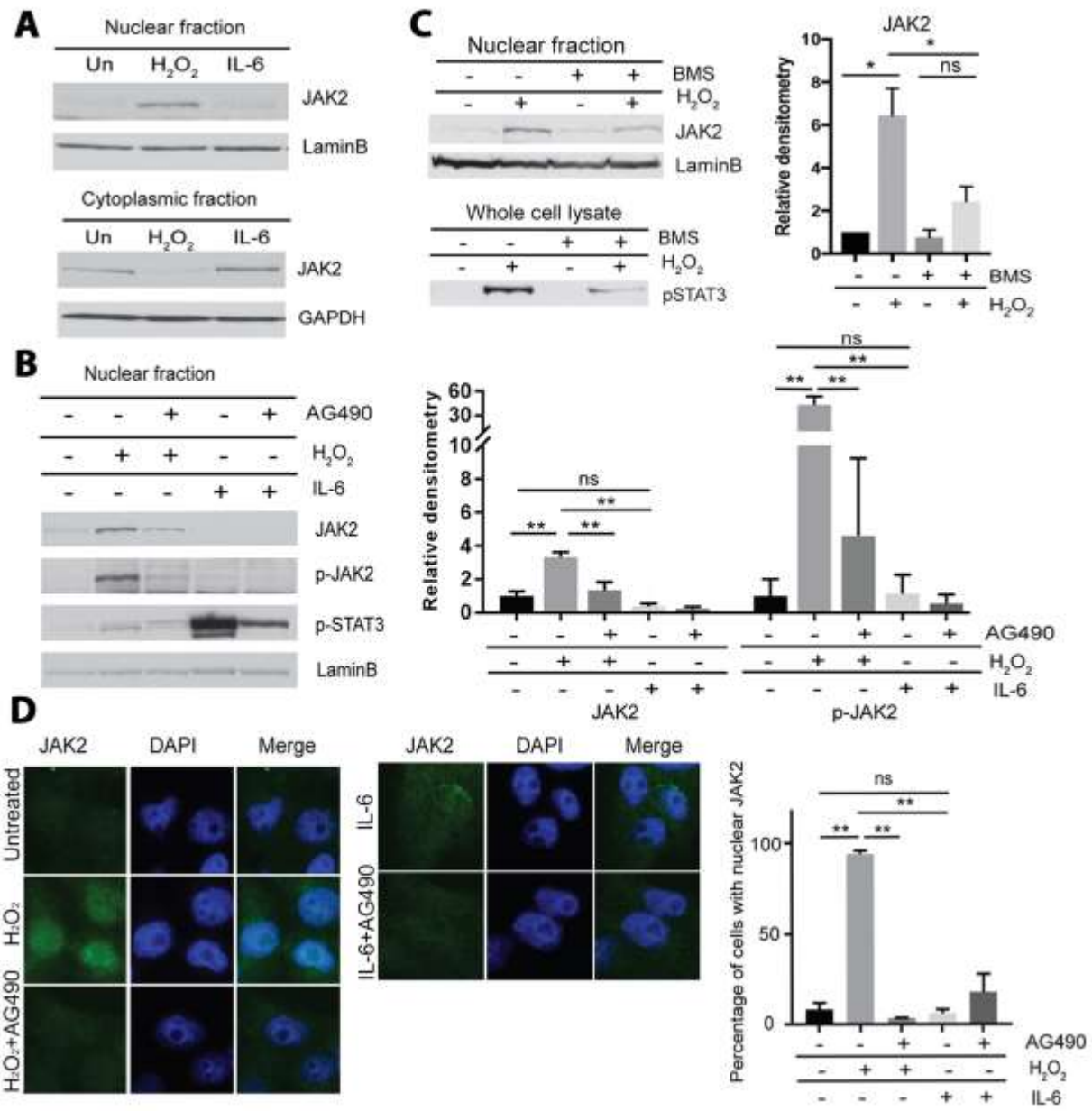

Figure 1. Oxidative damage induces catalytic activity-dependent JAK2 nuclear localization.

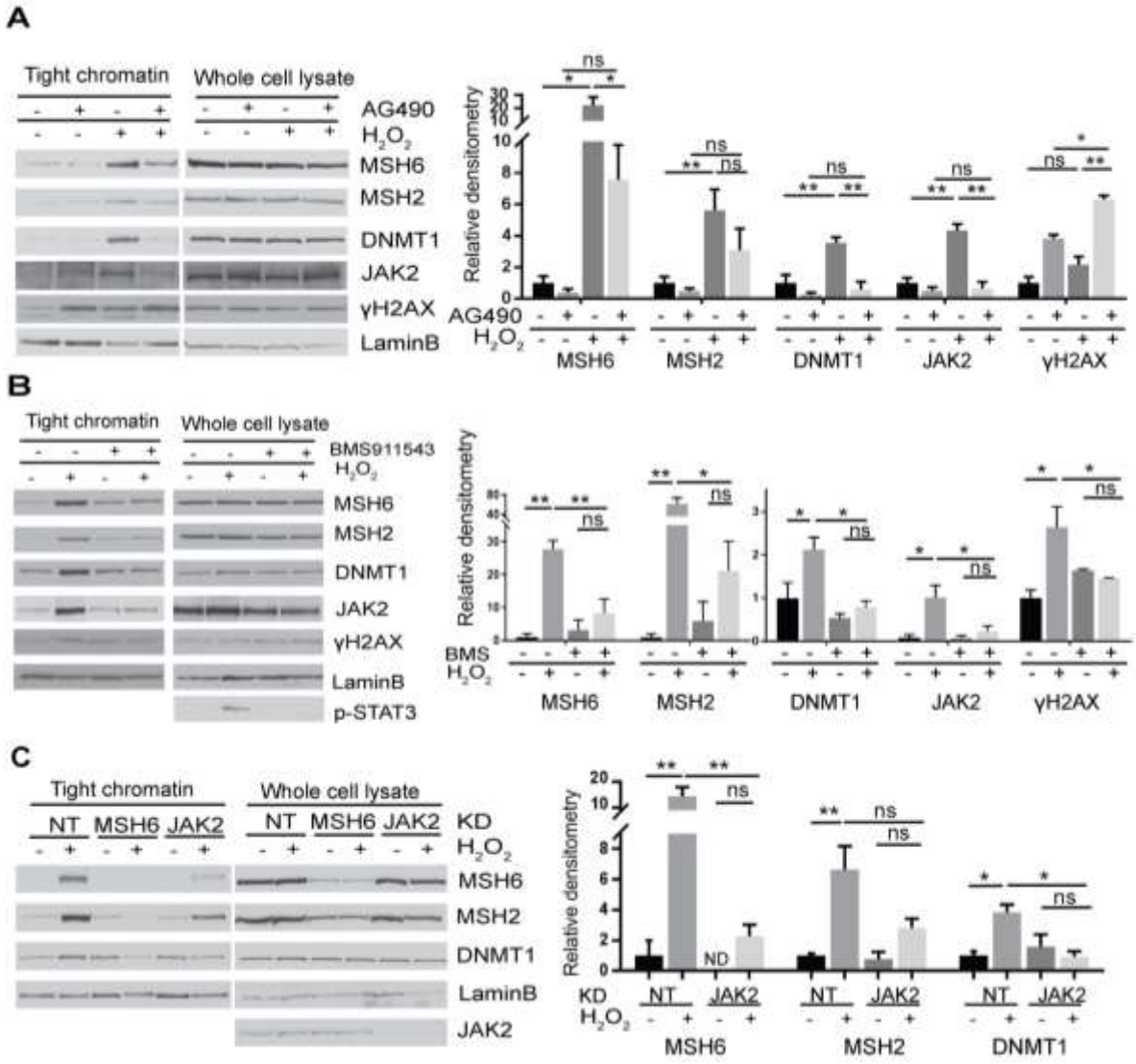

Figure 2. Inhibition of JAK2 alters oxidative damage-induced chromatin binding of MSH6 and DNMT1.

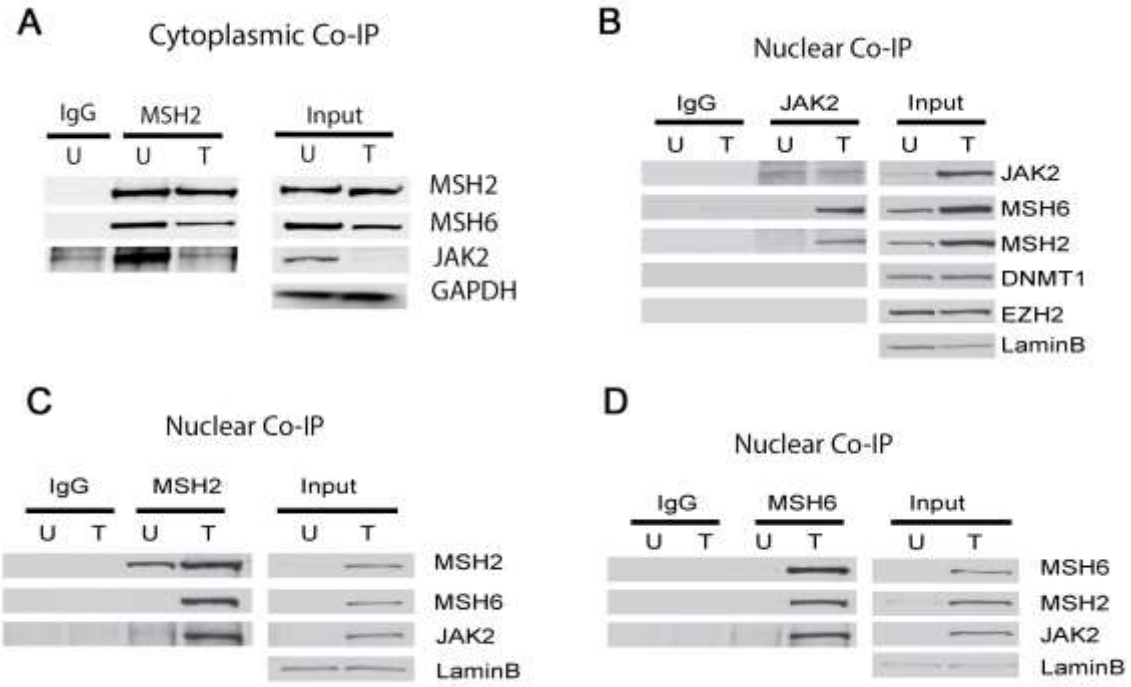

Figure 3. JAK2 interacts with MSH2 and MSH6 in the nucleus after oxidative damage.

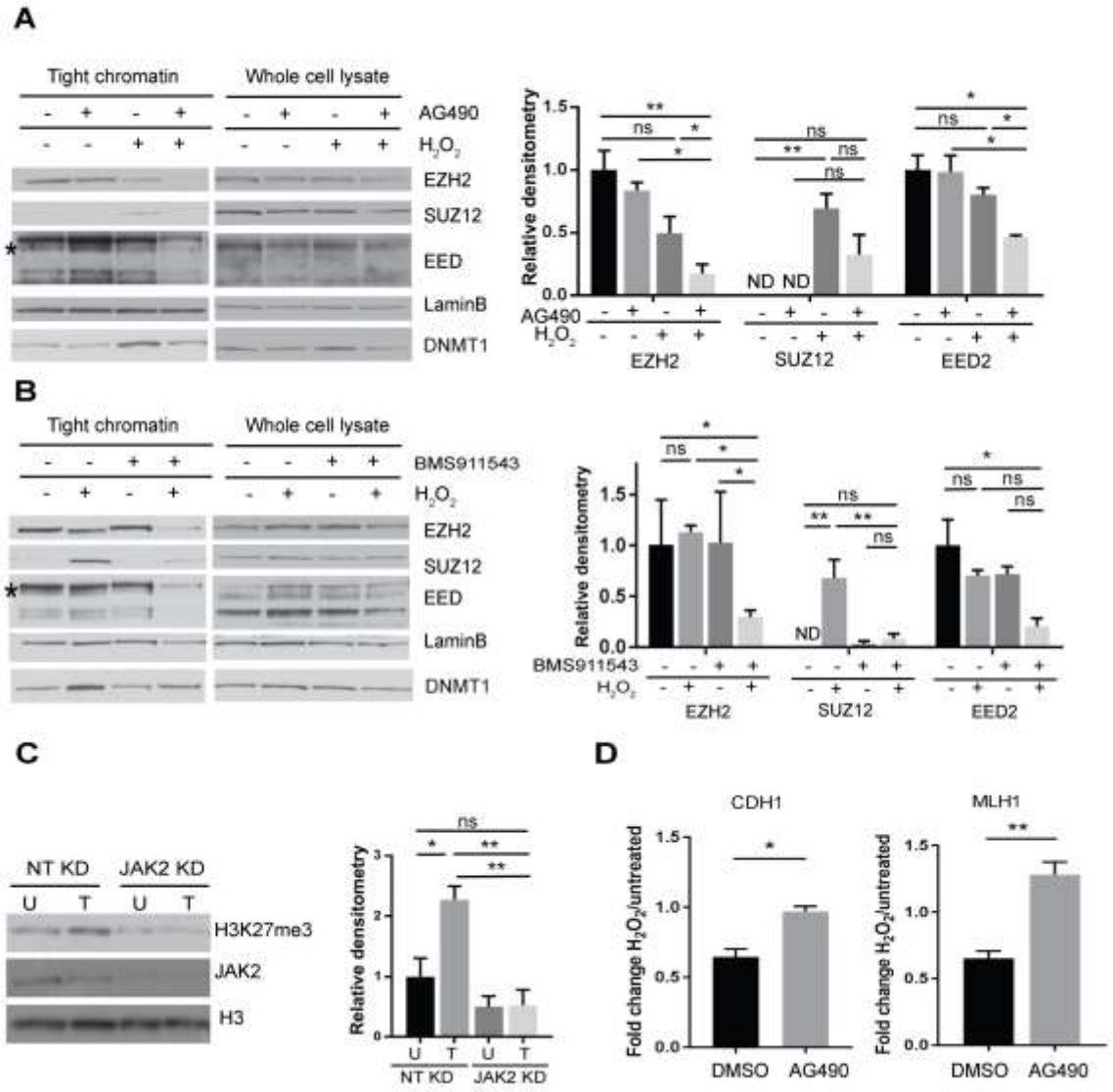

Figure 4. Inhibiting JAK2 alters the PRC2 response to oxidative damage.

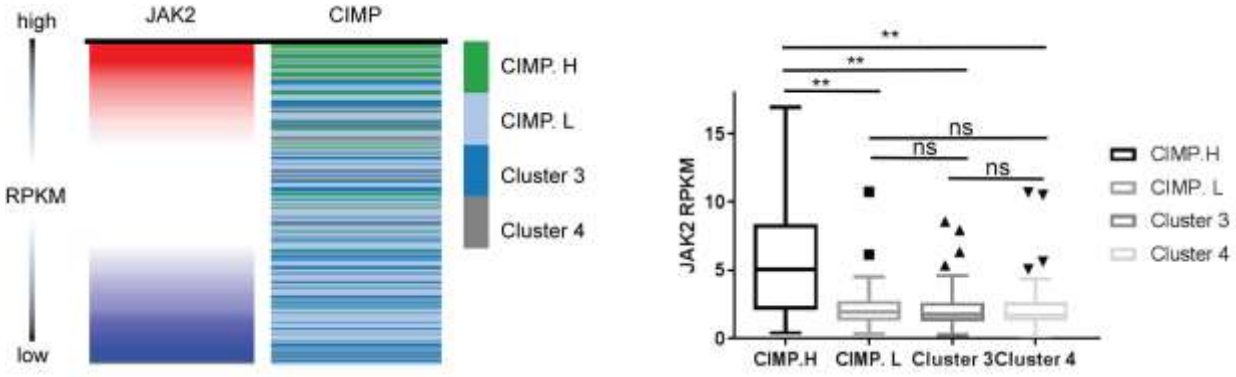

Figure 5. JAK2 expression is associated with CIMP status in human colorectal cancer.